Quantum teleportation of hybrid qubits and single-photon qubits using Gaussian resources

Soumyakanti Bose ●* and Hyunseok Jeong†

Department of Physics & Astronomy, Seoul National University, 1 Gwanak-ro, Gwanak-gu, Seoul 08826, Korea

We compare single-photon qubits and hybrid qubits as information carriers through quantum teleportation using a Gaussian continuous-variable channel. A hybrid qubit in our study is in the form of entanglement between a coherent state and a single photon. We find that hybrid qubits outperform photonic qubits when coherent amplitudes of the hybrid qubits are as low as $\alpha \lesssim 1$, while single-photon qubits yield better results for larger amplitudes. We analyze further the effect of photon losses and observe that the overall character of teleportation for different qubits remains the same although the teleportation fidelities are degraded by photon losses. Our work provides a comparative look at practical quantum information processing with different types of qubits.

I. INTRODUCTION

Quantum teleportation [1,2] provides a platform to transmit unknown quantum information at the cost of shared entanglement. It plays a central role in various quantum information processing tasks such as broadband communication [3], quantum computing [4–6], and secret key distillation [7]. Further developments provide feasibility of scalable quantum networks [8] leading to quantum internet [9]. So far, quantum teleportation based on photonic systems has been experimentally demonstrated and extensively analyzed for both discrete variable (DV) [10,11] and continuous variable (CV) [12,13] systems. While the teleportation of DV systems suffers from limited success probabilities [14], teleportation of CV states yields nonunit fidelities as it requires infinite squeezing that means an infinite amount of energy for perfect teleportation [2].

In order to circumvent the aforementioned difficulties, various attempts have been made using coherent-state qubits [15–19], ancillary states [20,21], squeezing operation [22,23], multiphoton qubits [24], and hybrid qubits [25,26]. Another idea is to use Gaussian resources to teleport qubits [27–29]. This approach has practical advantages that Gaussian quantum channels could readily be generated in a laboratory, and their characterizations are relatively straightforward [30,31]. On the other hand, it is more demanding to generate and analyze non-Gaussian channels [32–35]. Despite earlier studies on teleporting various types of qubits, an analysis of comparative performance of these qubits via CV channels remains an open issue.

In this article, we provide a partial answer to this query. Here, we critically investigate the teleportation of different types of qubits using an entangled Gaussian channel. To be specific, we focus on three different types of qubits: (a) the dual-rail single-photon qubit [6], (b) hybrid qubit of type

A that is entanglement between a single-photon state and a coherent state [36], and (c) hybrid qubit of type B that is entanglement between a single-photon state and superpositions of coherent sates [37]. As the entangled channel, we consider a pair of two-mode squeezed vacuum states (TMSVs), and analyze the performance of the CV-based teleportation [2].

To that end, we first obtain analytic expressions for the teleportation fidelity and elaborate our observation through various plots. Our results indicate that in the case of low amplitudes of the coherent states $\alpha \lesssim 1.0$ both types of the hybrid qubits, i.e., hybrid qubits (both types A and B) perform better than the single-photon qubit. Hybrid qubits are known to be useful for fault-tolerant quantum computing with error correction [25,38,39], and the best suggested value of α for hybrid qubits (type A) is ≈ 0.84 [39]. This suggests that the teleportation scheme investigated in this paper may result in advantages in terms of fault-tolerant quantum computing.

On the other hand, when the amplitudes are $\alpha \approx 1.0$, all three states offer the same fidelities. Nonetheless, the single-photon qubit outperforms hybrid qubits of both types as the coherent amplitude increases ($\alpha \gtrsim 1.0$). Next, we consider a realistic case when the channel undergoes symmetric photon losses and suffers from decoherence. We observe that the photon loss degrades the performance for all three types of qubits so that quantum teleportation does not succeed beyond a certain strength of loss. However, within the tolerable loss where quantum teleportation still prevails, the overall behavior remains similar to the ideal cases, i.e., without loss.

The present article is organized as follows. In Sec. II, we generalize the original protocol for continuous variable teleportation [2] to the case of a four-mode resource and a two-mode input state. In Sec. III, we show the relative comparison between the single-photon qubit and the hybrid qubits under ideal conditions. Section IV involves similar comparisons under the effects of photon losses. In Sec. V, we discuss various aspects of our results.

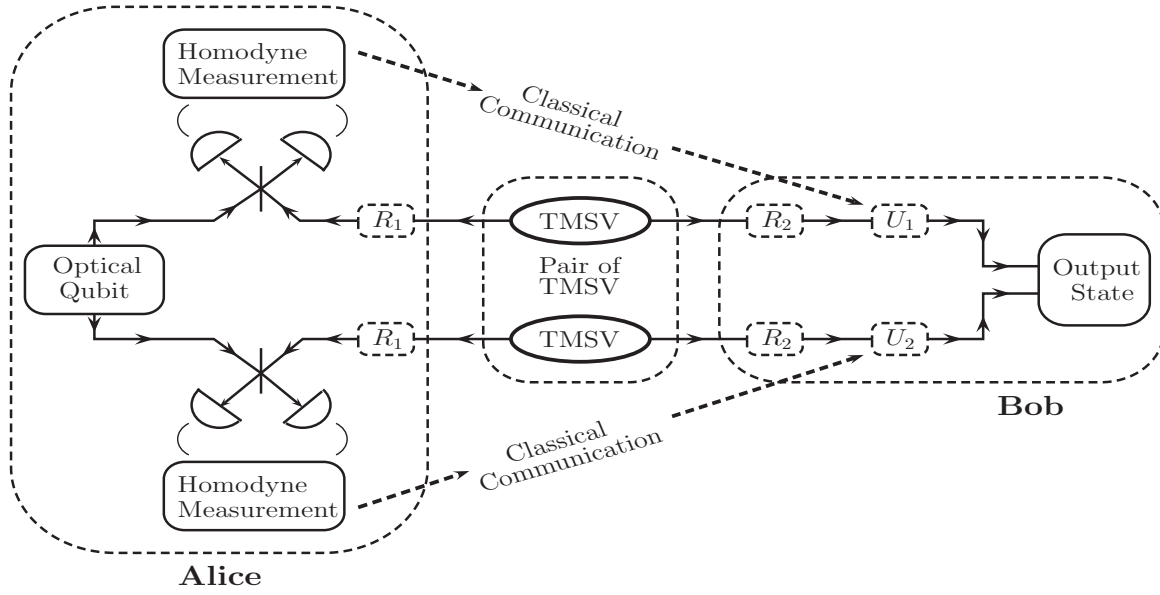* soumyabose@snu.ac.kr
† h.jeong37@gmail.com

FIG. 1. Schematic of teleportation of optical qubits using a pair-Gaussian state. First a pair of Gaussian states (TMSVs) are generated. Next, similar to the original protocol for CV teleportation [2], Alice makes the homodyne measurements on each of the modes of the optical qubit after mixing it with one of the incoming modes of two TMSVs in a 50:50 BS, separately. Then she communicates the results of the individual measurements to a distant party, say Bob classically. Subsequently, Bob makes unitary operations (based on the measurement results of Alice) on the remaining two modes of the pair of TMSVs and jointly recovers the input qubit state. Here R_1 and R_2 boxes are included just to explain the noisy (photon loss case). In case of no photon loss one simply takes $R_1 = R_2 = 0$. As the optical qubits, we have considered three different types such as dual rail single-photon qubit, hybrid qubit of type A, and hybrid qubit of type B (discussed in the text).

II. TELEPORTATION FIDELITY USING PAIR-GAUSSIAN CHANNEL

In the original protocol for CV teleportation [2], which involves a bipartite resource and a single-mode input, the fidelity F of teleportation could easily be evaluated in terms of the characteristic functions as [40,41]

$$F = \int \frac{d^2z}{\pi} \chi_{\text{in}}(z)\chi_{\text{res}}(z;z^*)\chi_{\text{in}}(-z), \tag{1}$$

where $\chi(z) = \text{Tr}[\rho D(z)]$, $D(z) = \exp[za^\dagger - z^*a]$. It is straightforward to extend this to a four-mode resource and a two-mode input state as

$$F = \iint \frac{d^2z_1}{\pi}\frac{d^2z_2}{\pi} \chi_{\text{res}}(z_1, z_2; z_1^*, z_2^*)$$
$$\times \chi_{\text{in}}(z_1, z_2) \times \chi_{\text{in}}(-z_1, -z_2). \tag{2}$$

Here, we consider the four-mode Gaussian channel to be a pair of TMSVs. In Fig. 1 we present the basic schematic of teleportation of optical qubits using a pair of TMSVs. TMSV states are described by the variance matrix $\Sigma = V \oplus V$, and V stands for the variance matrix of the TMSV given by

$$V = \begin{pmatrix} \eta & 0 & c & 0 \\ 0 & \eta & 0 & -c \\ c & 0 & \eta & 0 \\ 0 & -c & 0 & \eta \end{pmatrix} = \begin{pmatrix} \eta\mathbf{I} & c\sigma_z \\ c\sigma_z & \eta\mathbf{I} \end{pmatrix}, \tag{3}$$

where $\eta = \cosh(2r)/2$, $c = \sinh(2r)/2$, $\mathbf{I}$ is the 2×2 identity matrix, and σ_z is Pauli spin matrix. As a consequence, the resource state characteristic function in Eq. (2) is

$$\chi_{\text{res}}(z_1, z_2; z_1^*, z_2^*) = e^{-\vec{Z}^T \Sigma_c \vec{Z}}, \tag{4}$$

where $\vec{Z} = (z_1, z_1^*, z_2, z_2^*)^T$ and $\Sigma_c = \Sigma_c^1 \oplus \Sigma_c^2$ s.t. $\Sigma_c^i = \begin{pmatrix} 0 & \eta - c \\ \eta - c & 0 \end{pmatrix}$ $(i = 1, 2)$. Replacing $\chi_{\text{res}}(z_1, z_2; z_1^*, z_2^*)$ in (2), the fidelity for the two-mode input with the pair-Gaussian resource can be represented as

$$F = \int \frac{d\vec{Z}}{\pi^2} e^{-\vec{Z}^T \Sigma_c \vec{Z}} \chi_{\text{in}}(\vec{Z})\chi_{\text{in}}(-\vec{Z}). \tag{5}$$

We then explore quantum teleportation with a pair-Gaussian channel for the aforementioned types of qubits. It is known that in the case of qubits, quantum teleportation is successful when the fidelity is over the classical limit, i.e., $F > 2/3$ [42,43].

III. TELEPORTATION OF DIFFERENT TYPES OF QUBITS WITH PAIR-GAUSSIAN CHANNEL

In this article, we consider three different types of qubits. They are (a) dual-rail single-photon qubit (spq), (b) hybrid-qubit type A (hqA), and (c) hybrid-qubit type B (hqB) that can expressed as

$$|\psi_{\text{spq}}\rangle = \sqrt{p}|0, 1\rangle + \sqrt{1 - p}\, e^{i\phi}|1, 0\rangle, \tag{6}$$

$$|\psi_{\text{hqA}}\rangle = \sqrt{p}|0, \alpha\rangle + \sqrt{1 - p}\, e^{i\phi}|1, -\alpha\rangle, \tag{7}$$

$$|\psi_{\text{hqB}}\rangle = \sqrt{p}|0, \alpha_+\rangle + \sqrt{1 - p}\, e^{i\phi}|1, \alpha_-\rangle, \tag{8}$$

where $\alpha_\pm = (|\alpha\rangle \pm |-\alpha\rangle)/N_\pm$ are even (α_+) and odd (α_-) superpositions of coherent states with $N_\pm = 2(1 \pm e^{-2\alpha^2})$. It should be pointed out that hybrid qubits in the forms of Eq. (7) and Eq. (8) have been experimentally implemented in Ref. [36] and Ref. [37], respectively. These types of hybrid

entanglement are useful for quantum computation [25,38,39] as well as quantum communication [26,44–46].

A. Average fidelity of teleportation

The input states in Eqs. (6)–(8) are parametrized by two parameters p and ϕ. We thus write F in Eq. (5) as $F(p, \phi)$ in the present context. From an experimental point of view, it is natural to assume that parameters p and ϕ would vary during the trials. It is then imperative to look at the average behavior of the teleportation process. This could be accomplished by considering the fidelity averaged over all possible input states, i.e.,

$$F^{\text{av}} = \frac{1}{2\pi} \int dp \int d\phi \, F(p, \phi). \qquad (9)$$

Henceforth, we shall refer to Eq. (9) only while talking about fidelity, unless mentioned otherwise. Here we obtain an analytic expression for the teleportation fidelities for the input qubits as (Appendix A)

$$F_{\text{spq}}^{\text{av}} = \frac{4(4 + \Delta^2)}{(2 + \Delta)^2}, \qquad (10)$$

$$F_{\text{hqA}}^{\text{av}} = \frac{4}{3(2 + \Delta)^2}((2 + \Delta)^2 + (4 + \Delta^2)$$
$$+ (2 + \Delta)(\Delta e^{-\frac{8}{(2+\Delta)}\alpha^2} + 2e^{-\frac{4\Delta}{(2+\Delta)}\alpha^2})), \qquad (11)$$

$$F_{\text{hqB}}^{\text{av}} = \frac{8}{3(2 + \Delta)^2}\left(\left(1 + e^{-8\beta\alpha^2}\right)\left(\frac{1}{N_+^2} + \frac{1}{N_+ N_-} + \frac{1}{N_-^2}\right)\right.$$
$$+ e^{-4\alpha^2}\left(1 + e^{8\beta\alpha^2}\right)\left(\frac{1}{N_+^2} - \frac{1}{N_+ N_-} + \frac{1}{N_-^2}\right)$$
$$+ 4e^{-2\alpha^2}\left(\frac{1}{N_+^2} - \frac{(1)}{N_-^2}\right)$$
$$\left. + \frac{4\beta}{N_+ N_-}\left(e^{-4(1-2\beta)\alpha^2} - e^{-8\beta\alpha^2}\right)\right), \qquad (12)$$

where $\Delta = 4(\eta - c)$. The subscripts spq, hqA. and hqB represent single-photon qubit, hybrid qubit of type A, and hybrid qubit of type B, respectively.

In Fig. 2, we plot the comparisons of quantum teleportation fidelities for the single-photon qubit and the hybrid qubits with the pair-TMSV channel under the ideal condition without photon loss. As shown in the figures, hybrid qubits perform better as long as the coherent amplitude is $\alpha < 1$. When each type of qubit contains the average photon numbers of $\alpha \approx 1$, there is little distinction between the different types of qubits. With the increase in amplitude of the coherent state ($\alpha \gtrsim 1$) the single-photon qubit appears to yield better performance. It should also be noted that for all three types of qubits, quantum teleportation is achieved for the degree of squeezing is $r \gtrsim 1.0$.

B. Deviation in fidelity

While the average fidelity (9) describes the teleportation satisfactorily, it has been shown that higher order quantities like the *fidelity deviation* [47] play an important role in characterizing the teleportation process further. It is defined as the
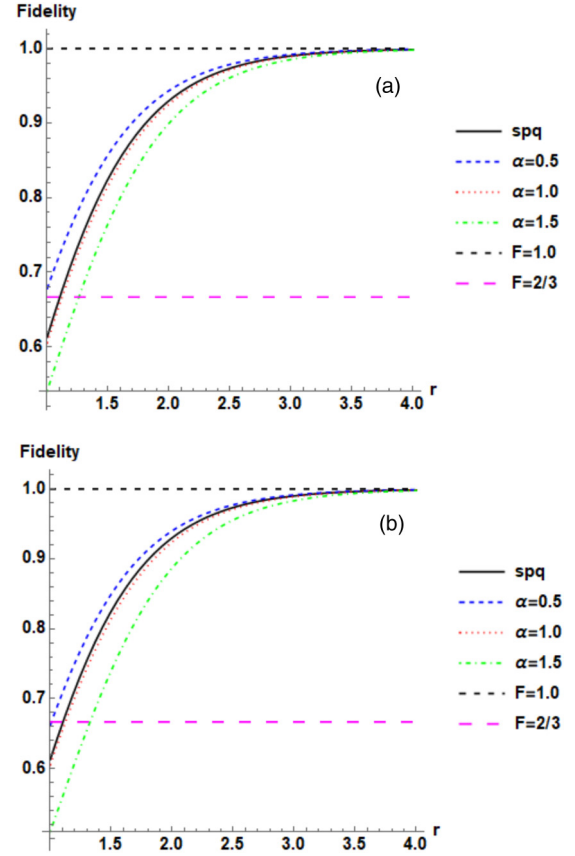

FIG. 2. (a) Teleportation fidelities of the single-photon qubit (solid curve) and hybrid qubits of type A against the squeezing degree r without photon loss. (b) Teleportation fidelities of the single-photon qubit (solid curve) and hybrid qubits of type B without photon loss.

uncertainty in fidelity, i.e.,

$$\Delta F = F_{\text{av}}^2 - (F_{\text{av}})^2, \qquad (13)$$

where averages are taken over p and ϕ as described in Eq. (9).

It may be noted that the fidelity of teleportation for the single-photon qubit is independent of p and ϕ (Appendix A) leading to the null result for the corresponding fidelity deviation. On the other hand, the *deviation* for the hybrid qubits depends only on the p (Appendix B). We obtain ΔF for hybrid qubits of types A and B in Appendix B, and plot in Fig. 3 the dependence of ΔF on the squeezing strength r for different values of α. We observe that, in general, at a given squeezing strength, the value of fidelity deviation is negligible compared to the respective average value for both types of hybrid qubits. This suggests that although deviation in fidelity is nonzero, average fidelity is enough to consider as a merit of teleportation for the hybrid qubits similar to the case of the single-photon qubit.

IV. TELEPORTATION OF QUBITS USING PAIR-GAUSSIAN CHANNEL UNDER PHOTON LOSS

In this section we consider teleportation of the qubits under decoherence. For the sake of simplicity we consider that the resource, i.e., the pair-Gaussian channel undergoes photon
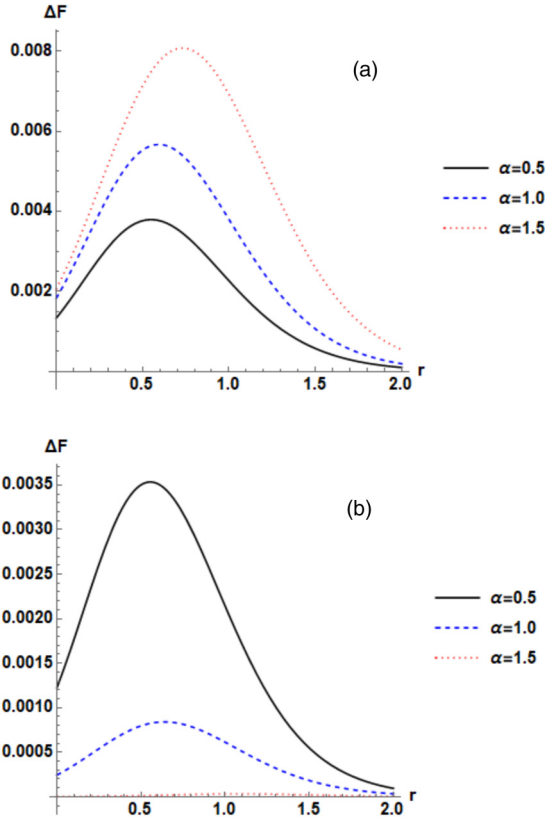
FIG. 3. (a) Deviation in teleportation fidelity ΔF for hybrid qubit type A against the squeezing degree r. (b) Deviation in teleportation fidelity for hybrid qubit type B against the squeezing degree. Various curves correspond to different values of α.
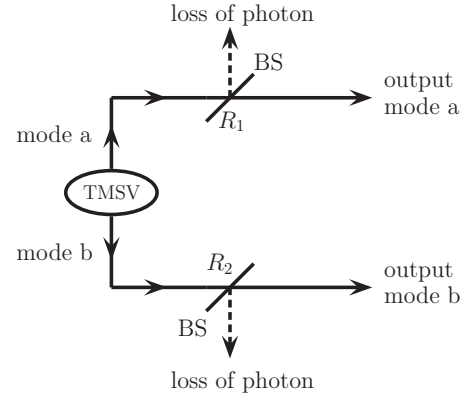

FIG. 4. Schematic of general photon loss on TMSV. BS stands for beam splitter. R_1 and R_2 are the loss parameters.

where $\eta' = \frac{1+2(1-R_1^2)\sinh^2 r}{2}$, $\zeta' = \frac{1+2(1-R_2^2)\sinh^2 r}{2}$, and $c' = \sqrt{(1-R_1^2)(1-R_2^2)}\cosh r \sinh r$. Corresponding fidelities in Eqs. (10), (11), and (12) could be accordingly obtained by replacing the variance matrix of Eq. (3) by that of Eq. (15).

A. Case 1: Asymmetric photon loss

Let us first consider a practical communication setup. Here, usually for a bipartite resource state, only one of the two modes (say the "communication mode") is sent to another distant party while the other mode (say the "laboratory mode") stays in the laboratory. As a consequence, the *laboratory mode* remains intact while the *communication mode* undergoes photon loss. Consequently, the elements of variance matrix (15) changes as $\eta' = \eta = (\cosh^2 r + \sinh^2 r)/2$, $\zeta = \frac{1+2(1-R^2)\sinh^2 r}{2}$, and $c' = (1-R^2)\cosh r \sinh r$.

In the asymmetric setup, only one mode suffers all photon losses while the photon losses are divided into two modes for the symmetric setup. Considering this observation, it is now important to note that in order to fairly compare the asymmetric loss with the symmetric loss of $R_1 = R_2 = R$ (see Fig. 4), we need to choose the asymmetric loss rate accordingly. For the symmetric case, if an input-mode field (either mode a or b in Fig. 4) of amplitude E travels for distance L, the output field amplitude is given by $\sqrt{1-R^2}E$, and it is the same for the other mode. However, in the asymmetric case, the corresponding traveling distance is $2L$ only for one field mode, and the output attenuated field amplitude would be $\sqrt{1-R^2}\sqrt{1-R^2}E = (1-R^2)E$. This leads to the loss rate for the asymmetric case as $R_1 = 0$ and $R_2 = \sqrt{2}R\sqrt{1-R^2/2}$. In this way, the total average photon losses remain the same for the two cases.

In Figs. 5 and 6, we plot the comparison of the single-photon qubit with hybrid qubits of types A and B, respectively. We compare for two different squeezing values as $r = 1.5$ and 2.0. We observe that the overall performances of the qubits remain the same except for the fact that the loss parameter (R) now restricts the experimentally available region over which teleportation is performed over the classical limit. As evident from the figures, teleportation fidelities drop down to the classical limit as the loss rate R increases.

loss. The effect of photon loss for a quantized electromagnetic wave could be modeled in terms of a passive beam splitter (BS). First the mode of interest passes through a passive BS with refectivity R while the other input arm of the BS is left at vacuum. Corresponding input-output mode relation for this BS could be written as

$$\begin{pmatrix} a_{\text{out}} \\ b_{\text{out}} \end{pmatrix} = \begin{pmatrix} \sqrt{1-R^2} & R \\ -R & \sqrt{1-R^2} \end{pmatrix} \begin{pmatrix} a_{\text{in}} \\ b_{\text{in}} \end{pmatrix}. \qquad (14)$$

Subsequently, discarding the output ancila modes (taking trace) leads to the effective photon loss on the input mode of the light. Here, $R = 1$ stands for complete photon loss.

To begin with, we first consider the general case where both the modes of the Gaussian state undergo photon loss parametrized by the respective losses, R_1 and R_2 (Fig. 4). This will enable us to analyze the two cases of interest.

(1) Asymmetric photon loss: Only one mode goes through photon loss while other remains intact.

(2) Symmetric photon loss: Both the modes undergo equal losses.

In a straightforward calculation the effect of this general photon loss on the input Gaussian state (3) leads to the change in the variance matrix as (Appendix C)

$$V_{\text{loss}}^{\text{gen}} = \begin{pmatrix} \eta'\mathbf{I} & c'\sigma_z \\ c'\sigma_z & \zeta'\mathbf{I} \end{pmatrix}, \qquad (15)$$

FIG. 5. Teleportation fidelities for the single-photon qubit and hybrid qubits of type A under asymmetric photon loss R.
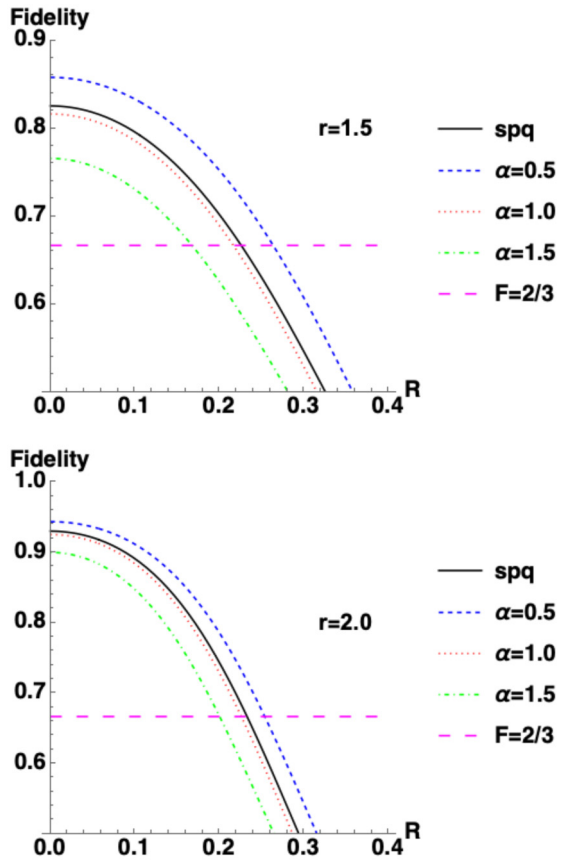

FIG. 6. Teleportation fidelities for the single-photon qubit and hybrid qubits of type B under asymmetric photon loss R.

B. Case 2: Symmetric photon loss

We further consider another situation where the resource state is generated at a third place at the center and is sent two equally distant parties of modes a and b. For the sake of simplicity, we consider that both the arms undergo the same losses as modeled by the condition of $R_1 = R_2 = R$. Evidently, under such loss the variance matrix (15) changes as $\eta' = \zeta' = \frac{1+2(1-R^2)\sinh^2 r}{2}$ and $c' = (1 - R^2)\cosh r \sinh r$.

In Figs. 7 and 8, we plot teleportation fidelities for the single-photon qubit and hybrid qubits under symmetric photon losses. For comparison, in line with the asymmetric case, we consider two different squeezing values as $r = 1.5$ and 2.0. Interestingly, we observe that the symmetric setup shows better performance in terms of the fidelity as shown in the figures.

V. CONCLUSION

We have analyzed quantum teleportation of single-photon qubits and hybrid qubits using a pair of Gaussian channels. We have considered two slightly different types of hybrid qubits. One is entanglement between a single photon and a coherent state, and the other is entanglement between a single photon and a coherent-state superposition. We note that the hybrid qubit of both types considered in this paper have been experimentally implemented [36,37] although their fidelities are yet limited. Our analysis is mostly centered around the
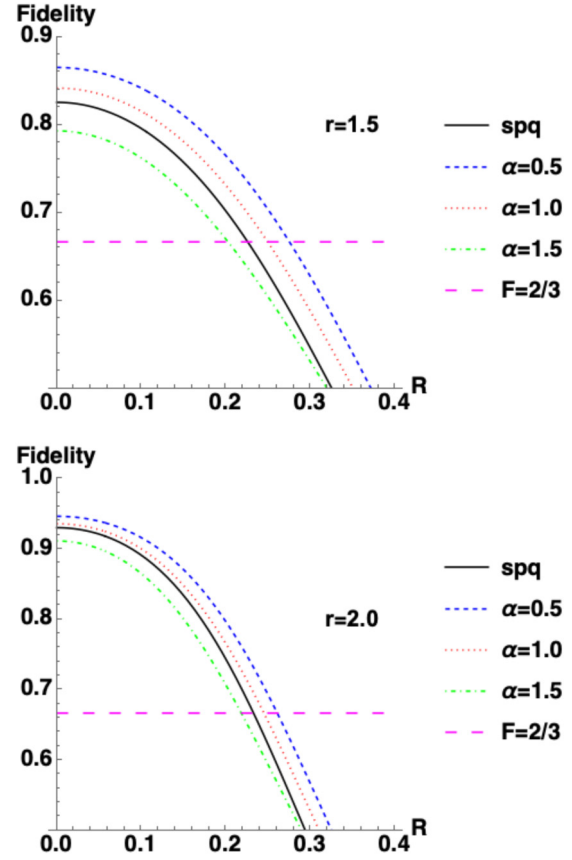
query of which type of qubit is better as an information carrier when a Gaussian channel is used for quantum teleportation.

To that end, we have shown that while the coherent amplitude is as low as $\alpha \lesssim 1$, both types of hybrid qubits yield better results than the single-photon qubit. On the other hand, as α increases, the single-photon qubit leads to better performance. We obtain similar values for all three types of qubits when $\alpha \approx 1$.

To apprehend the relative similarity between the different types of qubits for $\alpha \approx 1$, we have considered two nonclassical properties (not shown in the manuscript) of negativity of the Wigner function [48] and interference-based measure of macroscopic superpositions [49]. However, there seems to be no apparent similarity between the different types of qubits with respect to these attributes for $\alpha \approx 1$.

We have further analyzed the performance of qubit teleportation under the effect of photon loss. To that end, we have first described the analytical model for general photo-loss process where losses on both the modes are characterized by independent loss parameters R_1 and R_2. Subsequently, we have separately described two different cases of (a) the asymmetric one where only one of the modes undergoes photon loss while the other mode remains pure and (b) the symmetric case where both the modes undergo equal photon loss. We observe that although photon loss degrades the teleportation fidelities for both the symmetric and asymmetric cases, the symmetric case is more robust against loss under the same total amount
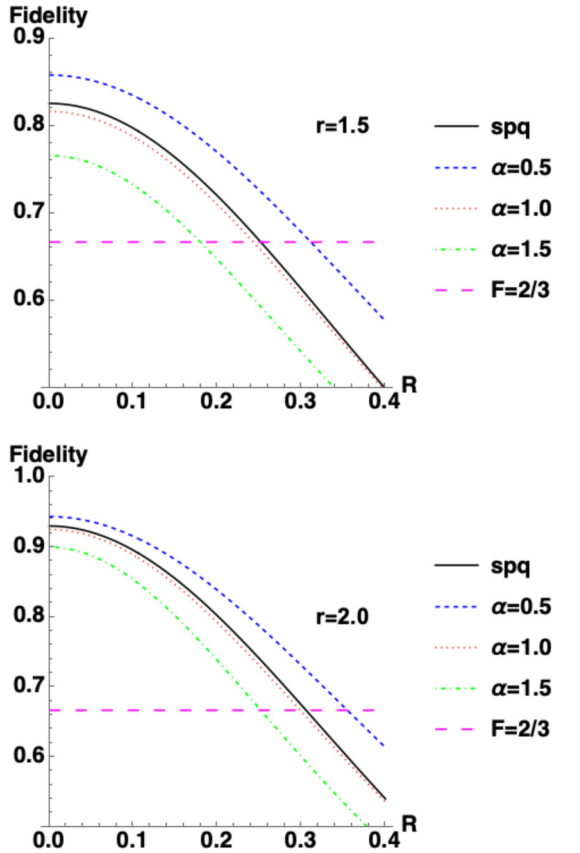
FIG. 7. Teleportation fidelities for the single-photon qubits and hybrid qubits of type A under symmetric photon loss.
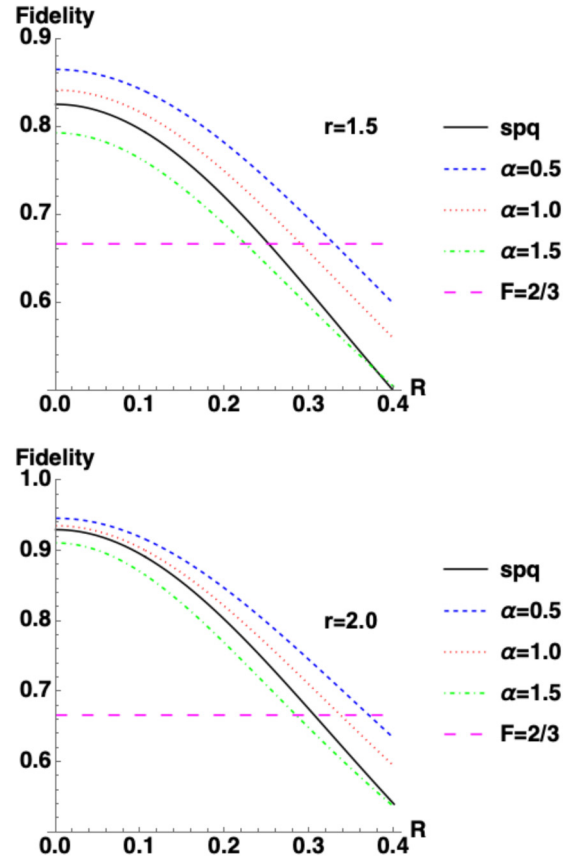

FIG. 8. Teleportation fidelities for the single-photon qubits and hybrid qubits of type B under symmetric photon loss.

of loss. It may imply that the entanglement structure of the Gaussian state is more fragile under the asymmetric loss, which deserves further investigation while it is beyond the scope of this work.

Hybrid qubits are useful for various applications including quantum computation [25,38,50] and quantum communication [51–55]. It is particularly advantageous for fault-tolerant quantum computing with error correction [38,39]. In Ref. [39], the authors suggested the best value of α for hybrid qubits (type A) to perform fault-tolerant quantum computing to be ≈ 0.84. We note that teleportation with a high fidelity is crucial for quantum computing schemes with hybrid qubits [25,38,39]. Here, we provide a comparative look at a practical quantum information processing task such as quantum teleportation of different types of qubits using Gaussian resources. Moreover, this article extends the schemes for Gaussian teleportation of qubits [27–29] from single-photon qubits to the case of hybrid qubits. This enables one to take advantage of the teleportation scheme studied in this paper in view of fault-tolerant quantum computing and accordingly choose the qubit of interest.

It is known that the fidelity is not always an ideal distance measure between two quantum states. In order to complement our argument, we have considered a second order quantity, called fidelity deviation [49], which is the uncertainty in fidelity considered over all possible combinations in input states. The deviations in fidelities for hybrid qubits appear to be negligible compared to the average fidelities for all values

of α. This may suggest that the average fidelity is a reasonable tool to characterize the teleportation using Gaussian resources.

It should be noted that hybrid qubits, which do not contain definite numbers of photons unlike dual-rail single-photon qubits, due to their uncertainty in photon numbers, produce unlocatable errors that cannot be readily noticed. In contrast, a dual-rail single-photon qubit contains definitely one photon, and its photon loss is relatively easy to be noticed at the photodetector. This difference should be considered with the quantitative results of this paper. We point out that the unlocatable errors for hybrid qubits can be corrected for quantum computing [25,38,39]. There are also further attempts to mitigate these effects for teleportation [56,57] while how to apply such schemes to our framework is an open question.

APPENDIX A: TELEPORTATION FIDELITY OF SINGLE-PHOTON QUBITS AND HYBRID QUBITS WITH A PAIR-GAUSSIAN CHANNEL

1. Teleportation fidelity for single-photon qubits

The characteristic function for the dual-rail single-photon qubit is given as

$$\chi_{\text{spq}}(\lambda_1, \lambda_2) = e^{-\frac{|\lambda_1|^2 + |\lambda_2|^2}{2}} (p\mathbf{L}_1(|\lambda_2|^2) + (1-p)\mathbf{L}_1(|\lambda_1|^2) - \sqrt{p(1-p)}[e^{i\phi}\lambda_1^*\lambda_2 + e^{-i\phi}\lambda_1\lambda_2^*]), \tag{A1}$$

where $\mathbf{L}_k(x)$ is the kth-order Laguerre polynomial. On the other hand the characteristic function for the resource state is given in Eq. (4). Consequently, considering the symmetry of the resource state, the fidelity for the single-photon qubit becomes

$$\begin{aligned}
F_{\text{spq}}(p, \phi) &= \iint \frac{d^2\lambda_1}{\pi} \frac{d^2\lambda_2}{\pi} \rho_{\text{res}}(\lambda_1, \lambda_2; \lambda_1^*, \lambda_2^*) \times \chi_{\text{spq}}(\lambda_1, \lambda_2) \times \chi_{\text{spq}}(-\lambda_1, -\lambda_2) \\
&= \iint \frac{d^2\lambda_1}{\pi} \frac{d^2\lambda_2}{\pi} e^{-\vec{\Lambda}^T(\Sigma_c + \frac{1}{2}\sigma_x \oplus \sigma_x)\vec{\Lambda}} \big([p^2 + (1-p)^2]\mathbf{L}_1^2(|\lambda_1|^2) + 2p(1-p)[\mathbf{L}_1(|\lambda_1|^2)\mathbf{L}_1(|\lambda_2|^2) + \cos(2\phi)\lambda_1^{*2}\lambda_2^2 \\
&\quad + |\lambda_1|^2|\lambda_2|^2] - 4\sqrt{p(1-p)}\cos(\phi)\mathbf{L}_1(|\lambda_1|^2)\lambda_1\lambda_2^*\big) \\
&= T_1 + T_2 + T_3 + T_4 + T_5 (\text{let}),
\end{aligned} \tag{A2}$$

where $\vec{\Lambda} = (\lambda_1, \lambda_1^*, \lambda_2, \lambda_2^*)^T$ and σ_x is the Pauli matrix. By using the generating function for the Laguerre polynomial in terms of parametric differentiation, $\mathbf{L}_n(xy) = \frac{1}{n!}\partial_a^n\partial_b^n[e^{ab+ax-by}]_{a,b=0}$, in a straightforward but tedious calculation, it could be shown that

$$T_1 = \frac{p^2 + (1-p)^2}{\det[M]}((1-2\beta)^2 + 4\beta^2); \quad T_2 = \frac{2p(1-p)}{\det[M]}(1-2\beta)^2; \quad T_3 = 0; \quad T_4 = \frac{2p(1-p)}{\det[M]}4\beta^2; \text{ and } T_5 = 0, \tag{A3}$$

where $4\det[M] = (2+\Delta)^2$, $\beta = \frac{2+\Delta}{4\det[M]} = \frac{1}{2+\Delta}$, and $\Delta = 4(\eta - c)$. Summing up all the terms and we obtain the fidelity as

$$F_{\text{spq}}(p, \phi) = \frac{(1-2\beta)^2 + 4\beta^2}{\det[M]} = \frac{4(4+\Delta^2)}{(2+\Delta)^2}, \tag{A4}$$

which is independent of p and ϕ.

2. Teleportation fidelity for hybrid qubit of type A (hqA)

The characteristic function of the hqA is given by

$$\chi_{\text{hqA}}(p, \phi) = e^{-\frac{|\lambda_1|^2 + |\lambda_2|^2}{2}} \big(pe^{-\alpha(\lambda_1 - \lambda_1^*)} + (1-p)e^{\alpha(\lambda_1 - \lambda_1^*)}\mathbf{L}_1(|\lambda_1|^2) - \sqrt{p(1-p)}e^{-2\alpha^2}[\lambda_2 e^{-i\phi}e^{\alpha(\lambda_1 + \lambda_1^*)} + \lambda_2^* e^{i\phi}e^{-\alpha(\lambda_1 + \lambda_1^*)}]\big), \tag{A5}$$

leading to the fidelity,

$$\begin{aligned}
F_{\text{hqA}}(p, \phi) &= \iint \frac{d^2\lambda_1}{\pi} \frac{d^2\lambda_2}{\pi} \rho_{\text{res}}(\lambda_1, \lambda_2; \lambda_1^*, \lambda_2^*) \times \chi_{\text{hqA}}(\lambda_1, \lambda_2) \times \chi_{\text{hqA}}(-\lambda_1, -\lambda_2) \\
&= \iint \frac{d^2\lambda_1}{\pi} \frac{d^2\lambda_2}{\pi} e^{-\vec{\Lambda}^T(\Sigma_c + \frac{1}{2}\sigma_x \oplus \sigma_x)\vec{\Lambda}} \big(p^2 + (1-p)^2\mathbf{L}_1^2(|\lambda_1|^2) + 2p(1-p)e^{2\alpha(\lambda_1 - \lambda_1^*)}\mathbf{L}_1(|\lambda_1|^2) \\
&\quad - 2p(1-p)e^{-4\alpha^2}[\lambda_2^2\cos(2\phi) - |\lambda_2|^2 e^{2\alpha(\lambda_1 + \lambda_1^*)}]\big) \\
&= T_1' + T_2' + T_3' - T_4' + T_5' \text{ (let)}.
\end{aligned} \tag{A6}$$

In straightforward calculation it could be shown that

$$T_1' = \frac{p^2}{\det[M]}; \quad T_2' = \frac{(1-p)^2}{\det[M]}((1-2\beta)^2 + 4\beta^2); \quad T_3' = \frac{2p(1-p)}{\det[M]}e^{-8\beta\alpha^2}(1-2\beta),$$

$$T_4' = 0; \quad T_5' = \frac{4p(1-p)e^{-4\alpha^2}}{\det[M]}\beta e^{8\beta\alpha^2}, \tag{A7}$$

leading to

$$F_{\text{hqA}}(p, \phi) = \frac{1}{\det[M]}(p^2 + (1-p)^2[(1-2\beta)^2 + 4\beta^2] + 2p(1-p)[(1-2\beta)e^{-8\beta\alpha^2} + 2\beta e^{-4\alpha^2}e^{8\beta\alpha^2}]). \tag{A8}$$

Averaging over p and ϕ and using the expressions for β and $\det[M]$, we get

$$F_{\text{hqA}}^{\text{av}} = \frac{4}{3(2+\Delta)^2}\big((2+\Delta)^2 + (4+\Delta^2) + (2+\Delta)[\Delta e^{-\frac{8}{(2+\Delta)}\alpha^2} + 2e^{-\frac{4\Delta}{(2+\Delta)}\alpha^2}]\big). \tag{A9}$$

3. Teleportation fidelity for hybrid qubit of type B (hqB)

Let us first consider the following quantities:

$$\chi_{\pm}(\lambda) = \langle \alpha_{\pm}|D(\lambda)|\alpha_{\pm}\rangle = \frac{e^{-|\lambda|^2/2}}{N_{\pm}}([e^{\alpha(\lambda-\lambda^*)} + e^{-\alpha(\lambda-\lambda^*)}] \pm e^{-2\alpha^2}[e^{\alpha(\lambda+\lambda^*)} + e^{-\alpha(\lambda+\lambda^*)}]),$$

$$\chi_{+-}(\lambda) = \langle \alpha_{+}|D(\lambda)|\alpha_{-}\rangle = \frac{e^{-|\lambda|^2/2}}{\sqrt{N_+ N_-}}([e^{\alpha(\lambda-\lambda^*)} - e^{-\alpha(\lambda-\lambda^*)}] + e^{-2\alpha^2}[e^{\alpha(\lambda+\lambda^*)} - e^{-\alpha(\lambda+\lambda^*)}]),$$

$$\chi_{-+}(\lambda) = \langle \alpha_{-}|D(\lambda)|\alpha_{+}\rangle = \frac{e^{-|\lambda|^2/2}}{\sqrt{N_+ N_-}}([e^{\alpha(\lambda-\lambda^*)} - e^{-\alpha(\lambda-\lambda^*)}] - e^{-2\alpha^2}[e^{\alpha(\lambda+\lambda^*)} - e^{-\alpha(\lambda+\lambda^*)}]). \quad \text{(A10)}$$

The characteristic function for the hybrid qubit of type B is then given as

$$\chi_{\text{hqB}}(p, \phi) = p\chi_+(\lambda_1)e^{-|\lambda_2|^2/2} + (1-p)e^{-|\lambda_2|^2/2}\mathbf{L}_1(|\lambda_2|^2) + \sqrt{p(1-p)}e^{-|\lambda_2|^2/2}(\lambda_2 e^{-i\phi}\chi_{-+}(\lambda_1) - \lambda_2^* e^{i\phi}\chi_{+-}(\lambda_1)). \quad \text{(A11)}$$

This leads to the fidelity for hqB,

$$\begin{aligned}
F_{\text{hqB}}(p, \phi) &= \iint \frac{d^2\lambda_1}{\pi}\frac{d^2\lambda_2}{\pi}\rho_{\text{res}}(\lambda_1, \lambda_2; \lambda_1^*, \lambda_2^*) \times \chi_{\text{hqB}}(\lambda_1, \lambda_2) \times \chi_{\text{hqB}}(-\lambda_1, -\lambda_2) \\
&= \iint \frac{d^2\lambda_1}{\pi}\frac{d^2\lambda_2}{\pi}e^{-\bar{\Lambda}^T\Sigma_c\bar{\Lambda}}e^{-|\lambda_2|^2}\Big(p^2\chi_+^2(\lambda_1) + (1-p)^2\chi_-^2(\lambda_1)\mathbf{L}_1^2(|\lambda_2|^2) + 2p(1-p)\chi_+(\lambda_1)\chi_-(\lambda_1)\mathbf{L}_1(|\lambda_2|^2) \\
&\quad + p(1-p)[\lambda_2^2 e^{-2i\phi}\chi_{-+}^2(\lambda_1) - \lambda_2^{*2}e^{2i\phi}\chi_{+-}^2(\lambda_1) - 2|\lambda_2|^2\chi_{+-}(\lambda_1)\chi_{-+}(\lambda_1)]\Big) \\
&= T_1'' + T_2'' + T_3'' + T_4'' + T_5'' - T_6'' \quad \text{(let)}, \quad \text{(A12)}
\end{aligned}$$

where we have made use of the following relations:

$$\chi_{\pm}(-\lambda) = \chi_{\pm}(\lambda); \quad \chi_{+-}(-\lambda) = -\chi_{+-}(-\lambda); \text{ and } \chi_{-+}(-\lambda) = -\chi_{-+}(\lambda). \quad \text{(A13)}$$

Similar to the previous cases it could be easily shown that

$$T_1'' = \frac{2p^2}{N_+^2\det[M]}\big([1 + e^{-8\beta\alpha^2}] + e^{-4\alpha^2}[1 + e^{8\beta\alpha^2}] + 4e^{-2\alpha^2}\big),$$

$$T_2'' = \frac{2(1-p)^2}{N_-^2\det[M]}\big([1 + e^{-8\beta\alpha^2}] + e^{-4\alpha^2}[1 + e^{8\beta\alpha^2}] - 4e^{-2\alpha^2}\big)\big((1-2\beta)^2 + 4\beta^2\big),$$

$$T_3'' = \frac{4p(1-p)}{N_+ N_-\det[M]}\big([1 + e^{-8\beta\alpha^2}] - e^{-4\alpha^2}[1 + e^{8\beta\alpha^2}]\big)(1-2\beta),$$

$$T_4'' = 0 = T_5'' \text{ \& } T_6'' = -\frac{4p(1-p)}{N_+ N_-\det[M]}\big([1 - e^{-8\beta\alpha^2}] + e^{-4\alpha^2}[1 - e^{8\beta\alpha^2}]\big)2\beta. \quad \text{(A14)}$$

Summing up all the terms we get

$$\begin{aligned}
F_{\text{hqB}}^{\text{av}} &= \frac{2}{\det[M]}\bigg(\big(1 + e^{-8\beta\alpha^2}\big)\Big(\frac{p}{N_+} + \frac{1-p}{N_-}\Big)^2 + e^{-4\alpha^2}\big(1 + e^{8\beta\alpha^2}\big)\Big(\frac{p}{N_+} - \frac{1-p}{N_-}\Big)^2 \\
&\quad + 4e^{-2\alpha^2}\Big(\frac{p^2}{N_+^2} - \frac{(1-p)^2}{N_-^2}\Big) + \frac{8\beta}{N_+ N_-}\big(e^{-4(1-2\beta)\alpha^2} - e^{-8\beta\alpha^2}\big)p(1-p)\bigg), \quad \text{(A15)}
\end{aligned}$$

which upon averaging leads to

$$\begin{aligned}
F_{\text{hqB}}^{\text{av}} &= \frac{8}{3(2+\Delta)^2}\bigg(\big(1 + e^{-8\beta\alpha^2}\big)\Big(\frac{1}{N_+^2} + \frac{1}{N_+ N_-} + \frac{1}{N_-^2}\Big) + e^{-4\alpha^2}\big(1 + e^{8\beta\alpha^2}\big)\Big(\frac{1}{N_+^2} - \frac{1}{N_+ N_-} + \frac{1}{N_-^2}\Big) \\
&\quad + 4e^{-2\alpha^2}\Big(\frac{1}{N_+^2} - \frac{(1)}{N_-^2}\Big) + \frac{4\beta}{N_+ N_-}\big(e^{-4(1-2\beta)\alpha^2} - e^{-8\beta\alpha^2}\big)\bigg). \quad \text{(A16)}
\end{aligned}$$

APPENDIX B: EXPRESSIONS OF FIDELITY DEVIATION FOR HYBRID QUBITS

Let us first consider the hybrid qubit of type A (hqA). Expression for the fidelity deviation for hqA could be obtained in the following way. The square of fidelity is easily obtained from Eq. (A8) by using the expressions for β and

$\det[M]$ as

$$F_{\mathrm{hqA}}^2(p,\phi) = \frac{16}{(2+\Delta)^4}\left(p^4 + (1-p)^4\frac{(4+\Delta^2)^2}{(2+\Delta)^4} + \frac{4p^2(1-p)^2}{(2+\Delta)^2}\left(\Delta e^{-\frac{8}{2+\Delta}\alpha^2} + 2e^{-\frac{4\Delta}{2+\Delta}\alpha^2}\right)^2 + 2p^2(1-p)^2\frac{4+\Delta^2}{(2+\Delta)^2},\right.$$

$$\left.\frac{4p^3(1-p)}{2+\Delta}\left(\Delta e^{-\frac{8}{2+\Delta}\alpha^2} + 2e^{-\frac{4\Delta}{2+\Delta}\alpha^2}\right) + \frac{4p(1-p)^3}{(2+\Delta)^2}\frac{4+\Delta^2}{(2+\Delta)^2}\left(\Delta e^{-\frac{8}{2+\Delta}\alpha^2} + 2e^{-\frac{4\Delta}{2+\Delta}\alpha^2}\right)\right), \tag{B1}$$

that leads to the average value,

$$\left(F_{\mathrm{hqA}}^2\right)_{\mathrm{av}} = \frac{1}{2\pi}\iint dp\,d\phi\,F_{\mathrm{hqA}}^2(p,\phi)$$

$$= \frac{16}{5(2+\Delta)^4}\left(1 + \frac{(4+\Delta^2)^2}{(2+\Delta)^4} + \frac{2}{3(2+\Delta)^2}\left(\Delta e^{-\frac{8}{2+\Delta}\alpha^2} + 2e^{-\frac{4\Delta}{2+\Delta}\alpha^2}\right)^2 + \frac{4+\Delta^2}{3(2+\Delta)^2}\right.$$

$$\left. + \frac{1}{2+\Delta}\left(\Delta e^{-\frac{8}{2+\Delta}\alpha^2} + 2e^{-\frac{4\Delta}{2+\Delta}\alpha^2}\right) + \frac{4+\Delta^2}{(2+\Delta)^3}\left(\Delta e^{-\frac{8}{2+\Delta}\alpha^2} + 2e^{-\frac{4\Delta}{2+\Delta}\alpha^2}\right)\right)$$

$$= \frac{16}{5(2+\Delta)^8}\left((2+\Delta)^4 + (4+\Delta^2)^2 + \frac{2(2+\Delta)^2}{3}\left(\Delta e^{-\frac{8}{2+\Delta}\alpha^2} + 2e^{-\frac{4\Delta}{2+\Delta}\alpha^2}\right)^2 + \frac{1}{3}(2+\Delta)^2(4+\Delta^2)\right.$$

$$\left. + (2+\Delta)\left((2+\Delta)^2 + (4+\Delta^2)\right)\left(\Delta e^{-\frac{8}{2+\Delta}\alpha^2} + 2e^{-\frac{4\Delta}{2+\Delta}\alpha^2}\right)\right). \tag{B2}$$

On the other hand, the square of average fidelity is given by

$$\left(F_{\mathrm{hqA}}^{\mathrm{av}}\right)^2 = \frac{16}{9(2+\Delta)^8}\left((2+\Delta)^4 + (4+\Delta^2)^2 + (2+\Delta)^2\left(\Delta e^{-\frac{8}{2+\Delta}\alpha^2} + 2e^{-\frac{4\Delta}{2+\Delta}\alpha^2}\right)^2 + 2(2+\Delta)^2(4+\Delta^2)\right.$$

$$\left. + 2(2+\Delta)\left((2+\Delta)^2 + (4+\Delta^2)\right)\left(\Delta e^{-\frac{8}{2+\Delta}\alpha^2} + 2e^{-\frac{4\Delta}{2+\Delta}\alpha^2}\right)\right), \tag{B3}$$

leading to the final result,

$$\Delta F_{\mathrm{hqA}} = \frac{16}{45(2+\Delta)^8}\left(4(2+\Delta)^4 + 4(4+\Delta^2)^2 - 7(2+\Delta)^2(4+\Delta^2) + (2+\Delta)^2\left(\Delta e^{-\frac{8}{2+\Delta}\alpha^2} + 2e^{-\frac{4\Delta}{2+\Delta}\alpha^2}\right)^2\right.$$

$$\left. - 2(2+\Delta)\left((2+\Delta)^2 + (4+\Delta^2)\right)\left(\Delta e^{-\frac{8}{2+\Delta}\alpha^2} + 2e^{-\frac{4\Delta}{2+\Delta}\alpha^2}\right)\right). \tag{B4}$$

Similarly, we obtain the results on fidelity deviation in the case of hybrid qubit type B. However, there seems to be no compact expression for ΔF_{hqB}. Consequently, we proceed with the numerical results.

APPENDIX C: CHANGE IN VARIANCE MATRIX OF THE PAIR-GAUSSIAN CHANNEL UNDER PHOTON LOSS

To evaluate the effect of photon loss, modeled by the BS operation and partial trace, we consider the extended vector composed quadrature of the system modes (a,b) and the ancilla modes (c,d) as $\vec{\zeta}_{\mathrm{ext}} = (x_a, p_a, x_b, p_b, x_c, p_c, x_d, p_d)^T$ leading to the input extended variance matrix of the four-mode system (i.e., including the ancilla modes) given as

$$V_{\mathrm{ext}}^{\mathrm{in}} = \begin{pmatrix} V & 0 & 0 \\ 0 & \mathbf{I}/2 & 0 \\ 0 & 0 & \mathbf{I}/2 \end{pmatrix} = \begin{pmatrix} \eta\mathbf{I} & c\sigma_z & 0 & 0 \\ c\sigma_z & \eta\mathbf{I} & 0 & 0 \\ 0 & 0 & \mathbf{I}/2 & 0 \\ 0 & 0 & 0 & \mathbf{I}/2 \end{pmatrix}. \tag{C1}$$

We first consider the action of a two-mode beam splitter (BS) with loss parameter R, ($U_{\mathrm{bs}}(R)$), on the local quadrature variables. Respective input-output relation is given by the matrix,

$$S_{\mathrm{bs},(2)} = \begin{pmatrix} \sqrt{1-R}\,\mathbf{I} & \sqrt{R}\,\mathbf{I} \\ \sqrt{R}\,\mathbf{I} & \sqrt{1-R}\,\mathbf{I} \end{pmatrix}. \tag{C2}$$

Accordingly, the four-mode BS matrix (for the modes a-c and b-d) with individual loss parameters R_1 and R_2 is given by

$$S_{\mathrm{bs},(4)} = \begin{pmatrix} \sqrt{1-R_1}\,\mathbf{I} & 0 & \sqrt{R_1}\,\mathbf{I} & 0 \\ 0 & \sqrt{1-R_2}\,\mathbf{I} & 0 & \sqrt{R_2}\,\mathbf{I} \\ \sqrt{R_1}\,\mathbf{I} & 0 & \sqrt{1-R_1}\,\mathbf{I} & 0 \\ 0 & \sqrt{R_1}\,\mathbf{I} & 0 & \sqrt{1-R_1}\,\mathbf{I} \end{pmatrix}. \tag{C3}$$

We know that if the quadrature variables are changed as $U_{\mathrm{bs}}: \vec{\zeta} \to S_{\mathrm{bs}}\vec{\zeta}$, then the variance matrix changes as $U_{\mathrm{bs}}: V \to S_{\mathrm{bs}}V S_{\mathrm{bs}}^T$, where "T" stands for transposition. Consequently, under the transformation $S_{\mathrm{bs},(4)}$, output extended variance matrix

will be

$$V_{\text{ext}}^{\text{out}} = S_{\text{bs},(4)} V_{\text{ext}}^{\text{in}} S_{\text{bs},(4)}^{T}$$

$$= \begin{pmatrix} (\eta(1-R_1)+R_1/2)\mathbf{I} & c\sqrt{(1-R_1)(1-R_2)}\sigma_z & \sqrt{R_1(1-R_1)}(-\eta+1/2)\mathbf{I} & -c\sqrt{R_2(1-R_1)}\sigma_z \\ c\sqrt{(1-R_1)(1-R_2)}\sigma_z & (\eta(1-R_2)+R_2/2)\mathbf{I} & -c\sqrt{R_1(1-R_2)}\sigma_z & \sqrt{R_2(1-R_2)}(-\eta+1/2)\mathbf{I} \\ \sqrt{R_1(1-R_1)}(-\eta+1/2)\mathbf{I} & -c\sqrt{R_1(1-R_2)}\sigma_z & (\eta R_1+(1-R_1)/2)\mathbf{I} & c\sqrt{R_1 R_2}\sigma_z \\ -c\sqrt{R_2(1-R_1)}\sigma_z & \sqrt{R_2(1-R_2)}(-\eta+1/2)\mathbf{I} & c\sqrt{R_1 R_2}\sigma_z & (\eta R_2+(1-R_2)/2)\mathbf{I} \end{pmatrix}.$$

$$(C4)$$

Evidently, the system variance matrix under photon loss is obtained, by considering the submatrix corresponding to the system modes, as

$$V_{\text{loss}}^{\text{gen}} = \begin{pmatrix} (\eta(1-R_1)+R_1/2)\mathbf{I} & c\sqrt{(1-R_1)(1-R_2)}\sigma_z \\ c\sqrt{(1-R_1)(1-R_2)}\sigma_z & (\eta(1-R_2)+R_2/2)\mathbf{I} \end{pmatrix}. \qquad (C5)$$

---

[1] C. H. Bennett, G. Brassard, C. Crepeau, R. Jozsa, A. Peres, and W. K. Wootters, Phys. Rev. Lett. **70**, 1895 (1993).

[2] S. L. Braunstein and H. J. Kimble, Phys. Rev. Lett. **80**, 869 (1998).

[3] P. van Loock, S. L. Braunstein, and H. J. Kimble, Phys. Rev. A **62**, 022309 (2000).

[4] D. Gottesman and I. L. Chuang, Nature (London) **402**, 390 (1999).

[5] R. Raussendorf and H. J. Briegel, Phys. Rev. Lett. **86**, 5188 (2001).

[6] E. Knill, R. Laflamme, and G. Milburn, Nature (London) **409**, 46 (2001).

[7] S. L. Braunstein and S. Pirandola, Phys. Rev. Lett. **108**, 130502 (2012).

[8] L. M. Duan, M. D. Lukin, J. I. Cirac, and P. Zoller, Nature (London) **414**, 413 (2001).

[9] H. J. Kimble, Nature (London) **453**, 1023 (2008).

[10] D. Bouwmeester, J.-W. Pan, K. Mattle, M. Eibl, H. Weinfurter, and A. Zeilinger, Nature (London) **390**, 575 (1997).

[11] X.-X. Xia, Q.-C. Sun, Q. Zhang, and J. W. Pan, Quantum Sci. Technol. **3**, 014012 (2018).

[12] A. Furusawa, J. L. Sørensen, S. L. Braunstein, C. A. Fuchs, H. J. Kimble, and E. S. Polzik, Science **282**, 706 (1998).

[13] S. L. Braunstein and P. van Loock, Rev. Mod. Phys. **77**, 513 (2005).

[14] N. Lutkenhaus, J. Calsamiglia, and K.-A. Suominen, Phys. Rev. A **59**, 3295 (1999).

[15] S. J. van Enk and O. Hirota, Phys. Rev. A **64**, 022313 (2001).

[16] H. Jeong, M. S. Kim, and J. Lee, Phys. Rev. A **64**, 052308 (2001).

[17] H. Jeong and M. S. Kim, Quantum Inf. Comput. **2**, 208 (2002).

[18] H. Jeong and M. S. Kim, Phys. Rev. A **65**, 042305 (2002).

[19] T. C. Ralph, A. Gilchrist, G. J. Milburn, W. J. Munro, and S. Glancy, Phys. Rev. A **68**, 042319 (2003).

[20] W. P. Grice, Phys. Rev. A **84**, 042331 (2011).

[21] F. Ewert and P. van Loock, Phys. Rev. Lett. **113**, 140403 (2014).

[22] H. A. Zaidi and P. van Loock, Phys. Rev. Lett. **110**, 260501 (2013).

[23] T Kilmer and S. Guha, Phys. Rev. A **99**, 032302 (2019).

[24] S.-W. Lee, K. Park, T. C. Ralph, and H. Jeong, Phys. Rev. Lett. **114**, 113603 (2015).

[25] S.-W. Lee and H. Jeong, Phys. Rev. A **87**, 022326 (2013).

[26] H. Kim, S.-W. Lee, and H. Jeong, Quantum Inf. Process. **15**, 4729 (2016).

[27] S. Takeda, T. Mizuta, M. Fuwa, P. van Loock, and A. Furusawa, Nature (London) **500**, 315 (2013).

[28] N. C. Menicucci, Phys. Rev. Lett. **112**, 120504 (2014).

[29] S. H. Lie and H. Jeong, Photon. Res. **7**, A7 (2019).

[30] R. Simon, N. Mukunda, and B. Dutta, Phys. Rev. A **49**, 1567 (1994).

[31] Arvind, B. Dutta, N. Mukunda, and R. Simon, Pramana **45**, 471 (1995).

[32] T. C. Ralph, A. P. Lund, and H. M. Wiseman, J. Opt. B: Quantum Semiclassical Opt. **7**, S245 (2005).

[33] J. H. Shapiro, Phys. Rev. A **73**, 062305 (2006).

[34] J. H. Shapiro and M. Razavi, New J. Phys. **9**, 16 (2007).

[35] J. Gea-Banacloche, Phys. Rev. A **81**, 043823 (2010).

[36] H. Jeong, A. Zavatta, M. Kang, S.-W. Lee, L. S. Costanzo, S. Grandi, T. C. Ralph, and M. Bellini, Nat. Photonics **8**, 564 (2014).

[37] O. Morin, K. Haung, J. Liu, H. L. Jeannic, C. Fabre, and J. Laurat, Nat. Photonics **8**, 570 (2014).

[38] S. Omkar, Y. S. Teo, and H. Jeong, Phys. Rev. Lett. **125**, 060501 (2020).

[39] S. Omkar, Y. S. Teo, S.-W. Lee, and H. Jeong, Phys. Rev. A **103**, 032602 (2021).

[40] A. V. Chizhov, L. Knoll, and D. G. Welsch, Phys. Rev. A **65**, 022310 (2002).

[41] P. Marian and T. A. Marian, Phys. Rev. A **74**, 042306 (2006).

[42] R. Horodecki, M. Horodecki, and P. Horodecki, Phys. Lett. A **222**, 21 (1996).

[43] N. Gisin, Phys. Lett. A **210**, 157 (1996).

[44] K. Park, S.-W. Lee, and H. Jeong, Phys. Rev. A **86**, 062301 (2012).

[45] H. Jeong, S. Bae, and S. Choi, Quant. Info. Proc. **15**, 913 (2016).

[46] S. Choi, S. H. Lee, and H. Jeong, Phys. Rev. A **102**, 012424 (2020).

[47] J. Bang, J. Ryu, and D. Kaszlikowski, J. Phys. A: Math. Theor. **51**, 135302 (2018).

[48] A. Kenfack and K. Zyczkowski, J. Opt. B: Quantum Semiclass. Opt. **6**, 396 (2004).

[49] C.-W. Lee and H. Jeong, Phys. Rev. Lett. **106**, 220401 (2011).

[50] P. van Loock, W. J. Munro, K. Nemoto, T. P. Spiller, T. D. Ladd, S. L. Braunstein, and G. J. Milburn, Phys. Rev. A **78**, 022303 (2008).

[51] Y.-B. Sheng, L. Zhou, and G.-L. Long, Phys. Rev. A **88**, 022302 (2013).

[52] Y. Lim, J. Joo, T. P. Spiller, and H. Jeong, Phys. Rev. A **94**, 062337 (2016).

[53] R. C. Parker, J. Joo, M. Razavi, and T. P. Spiller, J. Opt. **19**, 104004 (2017).

[54] R. C. Parker, J. Joo, and T. P. Spiller, Proc. R. Soc. A **476**, 2243 (2020).

[55] J. Wen, I. Novikova, C. Qian, C. Zhang, and S. Du, Photonics **8**, 552 (2021).

[56] B. W. Walshe, B. Q. Baragiola, R. N. Alexander, and N. C. Menicucci, Phys. Rev. A **102**, 062411 (2020).

[57] T. Hillmann, F. Quijandría, A. L. Grimsmo and G. Ferrini, arXiv:2108.1009.